Ground state of $S = \frac{1}{2}$ Triangular Lattice Heisenberg-like Antiferromagnet Ba₃CoSb₂O₉ in an out-of-plane magnetic field

X. Z. Liu

[1] *Guangdong Key Laboratory of Magnetoelectric Physics and Devices,*
School of Physics, Sun Yat-sen University, Guangzhou 510275, China
[2] *Centre for Physical Mechanics and Biophysics, School of Physics,*
Sun Yat-sen University, Guangzhou 510275, China
[3] *Center for Neutron Science and Technology, School of Physics,*
Sun Yat-sen University, Guangzhou 510275, China

O. Prokhnenko, M. Bartkowiak, and A. Gazizulina

Helmholtz-Zentrum Berlin für Materialien und Energie GmbH,
Hahn-Meitner-Platz 1, D-14109 Berlin, Germany

D. Yamamoto

Department of Physics, College of Humanities and Sciences, Nihon University, Tokyo 156-8550, Japan

A. Matsuo and K. Kindo

Institute for Solid State Physics, University of Tokyo, Kashiwa, Chiba 277-8581, Japan

K. Okada, N. Kurita, and H. Tanaka

Department of Physics, Tokyo Institute of Technology, Oh-okayama, Meguro-ku Tokyo 152-8551, Japan
(Dated: December 10, 2022)

Spin-$\frac{1}{2}$ triangular lattice Heisenberg antiferromagnet has been accepted as an ideal system for quantum magnetism studies and quantum simulations. This system, for which the classical ground state degeneracy is lifted by quantum fluctuations, exhibits a series of novel spin structures for a field applied in-plane and out-of-plane. It has been found that both anisotropy and interlayer interaction play an important role in stabilization of the spin configurations in a magnetic field. Conversely, the phase transitions and spin-state evolution in a field along various orientations can provide a deep insight into physics of the triangular lattice Heisenberg antiferromagnet system. While the quantum magnetization process in an in-plane field has been studied extensively, the ground state evolution in the field along the c-axis requires further investigation. Here we performed high field magnetization and neutron scattering investigations on a model system of spin-$\frac{1}{2}$ triangular lattice Heisenberg antiferromagnet Ba₃CoSb₂O₉ with field along c-axis and with a small offset angle. For $H \parallel c$, the magnetization reveals a narrow plateau prompting a UUD-like phase, which could be suppressed by tilting the field away from the c-axis. From the neutron data, a phase transition $\mu_0 H_{c1} \sim 12$T is detected and interpreted as a transition from an umbrella to a coplanar phase. Around about 22.5T ($\mu_0 H_{c2}$) for $H \parallel c$, another transition is observed which might be attributed to a transition between the coplanar V and V' phases based on a comparison with the calculations and previous results. Theoretical calculations using the large-size cluster mean-field plus scaling method predicts a similar phase evolution as the previous semiclassical analysis, and agree with experiment well. The discrepancies between theory and experiment are also discussed, suggesting the physics of a triangular lattice Heisenberg antiferromagnet in a field along c-axis has not been fully unraveled.

PACS numbers: 75.10.Jm, 75.25.-j, 75.40.Mg

I. INTRODUCTION

Frustrated magnetism is one of central topics in condensed matter physics[1] giving rise to many interesting novel concepts, such as e.g. quantum spin liquid[2] and quantum magnetization plateau[3–7]. In the latter case, quantum fluctuations lift the accidental degeneracies of classic limit and result in novel ground state and excitations. A remarkable model system here is the spin $S = \frac{1}{2}$ triangle lattice Heisenberg antiferromagnet (TLHAF). In zero field it forms a 120° or so-called Y-type structure below Neél temperature [8–14],

due to the zero point energy. In an in-plane field, it was demonstrated that a quantum magnetization plateau at one third of saturated magnetization ($1/3M_s$) associated with an up-up-down(UUD) spin configuration is stabilized by quantum fluctuations and easy-plane anisotropy. This was long predicted by theories and recently observed in various real systems. Several representative compounds include Cs₂CuBr₄[15, 16], Ba₃CoSb₂O₉ [17, 18], CsCuCl₃[19, 20].

All these materials exhibit a $1/3M_s$ quantum magnetization plateau resulting from quantum fluctuations rather than thermal fluctuations at low temperatures. In

a perfect TLHAF system, the ground state and excitations are mainly determined by the intralayer interaction, whereas in the real systems they can be affected by anisotropy and interlayer interactions. Already the earliest experimental systems Cs_2CuBr_4 and $CsCuCl_3$ were found to show an evidence of quantum magnetization plateau. However, the magnetic properties of these compounds are complicated because of a relative low orthorhombic structural symmetry and Dzyaloshinskii-Moriya (D-M) interactions[15], due to the Jahn-Teller distortion of Cu^{2+} cation. On the other hand, the compound $Ba_3CoSb_2O_9$ is found to almost perfectly approximate TLHAF. It crystallizes in a layered structure with a high symmetric hexagonal lattice (SGP: $P6_3/mmc$) without the disruption caused by the D-M interactions. Co^{2+}-ions form regular triangle layers isolated by two neighboring nonmagnetic Sb^{5+} triangle layers which enables a weak interlayer interaction. The Co^{2+}-ions can be safely treated as an effective $S = \frac{1}{2}$ ions due to a well isolated Kramers doublet ground state for T<50K[17]. The intraplane interaction between adjacent Co^{2+} is determined to be $J \sim 19K$, while the interlayer interaction is more than one order of magnitude weaker, which reduces the Néel temperature associated with 3D long range ordering down to $T_N = 3.8K$[21]. The interlayer interaction J' is estimated to be about $J'/J = 0.052$ by neutron scattering[22], and 0.026 by ESR measurement[23]. ESR measurements provide very close g-factors for both in-plane and out-of-plane field directions. Both inelastic neutron scattering (INS)[24] and theoretical work [25] support a slightly smaller interaction out-of-plane than in-plane, manifesting an easy plane XXZ system. Although it remains slightly anisotropic, $Ba_3CoSb_2O_9$ still closely approximate to a perfect TLHAF model and could serve as a platform for investigating low dimensional quantum magnetism.

It is therefore interesting to study the field dependence of the spin structure of $Ba_3CoSb_2O_9$ in the entire field range up to saturation along various field directions. The ground state with the magnetic field applied in the ab-plane has been investigated by a number of experimental techniques such as magnetization[17, 23], ESR[23], sound velocity[26], NMR[27], calorimetry[28], and neutron scattering [22, 24, 29]. As a result, a consistent phase diagram has been established. Especially, an UUD spin configuration in the field range for $0.30H_s < H < 0.47H_s$ corresponding to $\frac{1}{3}M_s$ magnetization plateau and $V - V'$ transition around $0.7H_s$ associated with a magnetization kink have been well reproduced by various techniques [22, 30] and are in good agreement with the theoretical calculations[25, 31–34]. The corresponding collinear UUD and coplanar V and V' phases are depicted in Fig.4(c-e). However, the spin configuration in very high fields has rarely been probed directly. Recently, we examined the spin ground state for field in the ab-plane up to 26 T by neutron scattering[30]. By contrast, the ground state of $Ba_3CoSb_2O_9$ for the magnetic field applied out-of-plane received less atten-

tion and number of deviations between the experiments and the theories exist up to date[27, 28]. The evolution of spin configurations with the field has been studied by magnetization[17, 19, 23, 27, 28], NMR[27], calorimetry[28]. The experimentally observed dependences are frequently inconsistent with theoretical prediction. Although some knowledge about phase transitions is obtained from these measurements, the information about the real spin alignment for each phase is still missing. Thus physics of the TLHAF with interlayer interaction and in-plane anisotropy is far from being completely understood and more efforts from both theory and experiment are required.

Based on the semiclassical analysis, a different sequence of magnetic transitions as a function of out-of-plane magnetic field has been predicted as compared to that for the in-plane field [27]. In contrast to a distorted Y-phase for the in-plane fields, at low fields for $H \parallel c$, an umbrella phase with in-plane components of magnetic moments being rotated by 120° is stabilized by the in-plane anisotropy up to a field $\mu_0 H_{c1}$. The semiclassical analysis predicts no UUD phase for $H \parallel c$. Instead, the umbrella phase should be followed by a transition to the V phase at $\mu_0 H_{c1} \sim 12$T. At fields higher than about 22T at ~2 K, another high field state is predicted and experimentally observed. Such a phase transition has been ascribed to the weak but finite interlayer interaction as revealed by both the calculations and experiments though the nature of the high field phase has not been unambiguously identified. According to the semiclassical calculations performed for a $H \parallel c$ and the cluster mean field plus scaling (CMF+S) calculations performed for in-plane field, the high field phase above 22 T can be either a V′-phase or Ψ-phase, appearing via first or second order transition, respectively[25, 27, 28, 30]. Recently this transition was also disclosed by NMR and calorimetry measurements. The NMR experiment showed a kink of local field strength of $^{135,137}Ba$ nucleus in an out-of-plane field [27] while the calorimetry measurements revealed a phase transition around 22 T at a comparable temperature[28]. However, due to experimental difficulties in detecting the microscopic spin alignment in high fields, we are still lacking a systematic experimental verification of the spin configurations in high fields along the c-axis. The EXtreme Environment Diffractometer (EXED) at Helmholtz-Zentrum Berlin (HZB) featured a unique horizontal high-field magnet capable of reaching fields up to 26 T and provided unprecedented opportunity for this task before its shutdown in 2019. To address these unsolved issues and shed some light on the ground state of TLHAF in an out-of-plane field, we conducted this work.

II. EXPERIMENTAL

$Ba_3CoSb_2O_9$ single crystal used for neutron scattering is the same sample which had been used in our previous
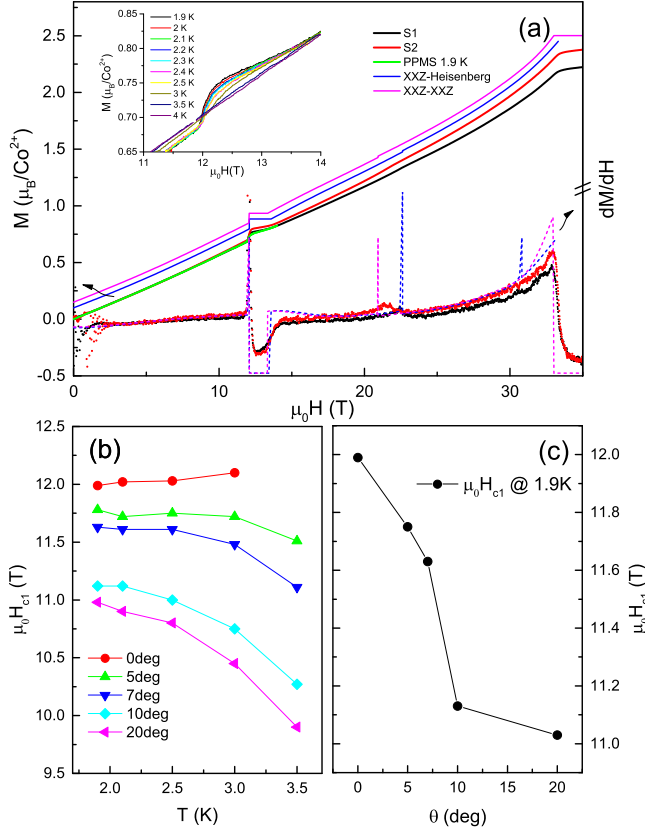
FIG. 1: (a) The magnetization (and its first derivative, dM/dH) measured in both pulsed and dc fields applied along the c-axis, where the samples S1 and S2 are taken from different batches. The calculated curve derived from the CMF+S calculation using isotropic (blue) and anisotropic (magenta) interlayer interactions (see Section IV) are also shown with an intentional offset of $0.1\mu_B/Co^{2+}$ and $0.15\mu_B/Co^{2+}$ for better visibility. The upper inset displays the transition around 12 T at various temperatures while the right axis presents the first derivative for both measured and calculated results shown in left axis. (b) The transition field around 12 T as a function of temperature. (c) The transition field around 12 T as a function of field orientation at 1.9 K.

work[30]. Its dimensions are $4 \times 4 \times 4mm^3$ and weight is 0.42 g. For details of crystal growth refer to Ref. [35]. Magnetization measurements in DC fields up to 14T have been performed using Physical Properties Measurement System (Quantum Design) at HZB. The sample was from the same batch as that used in neutron diffraction experiment. The angular dependence has been obtained by regluing the sample manually. The estimated orientation error is $2 \sim 3°$. The magnetization processes of two other samples from the different batches were measured in pulsed high-field magnetic fields up to 35 T for magnetic field $H \parallel c$ axis at $T = 1.3$ K. Here, a plate-
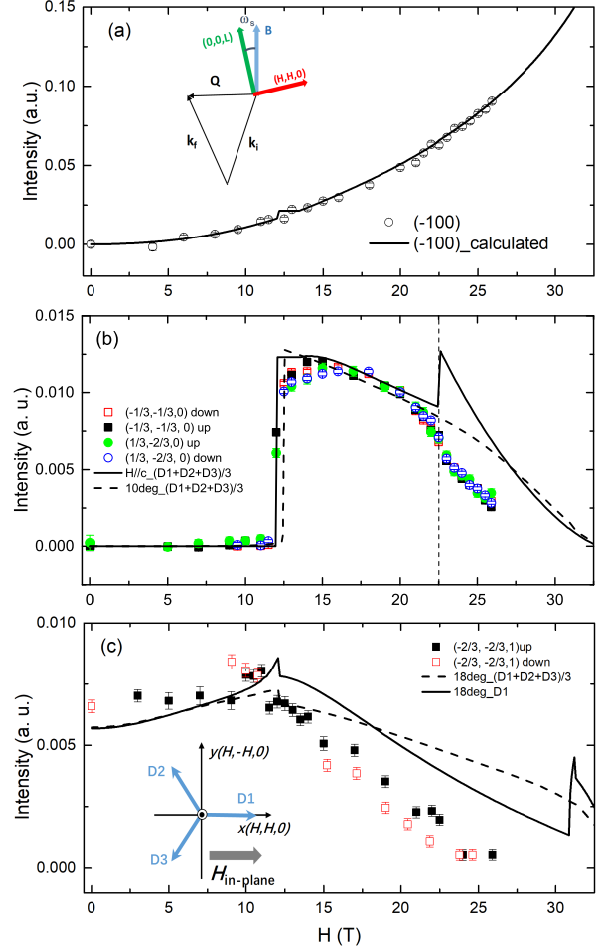

FIG. 2: (Color online) The intensity (symbols) of measured reflections as function of field: (a) (-1, 0, 0), (b) (-1/3, -1/3, 0) and (1/3, -2/3, 0), and (c) (-2/3, -2/3, 1). The inset in (a) displays a schematic view of the experiment geometry. The lines are the results derived from CMF + S calculations. The intensities of the reflections with $L = 0$ in (a) and (b) are calculated with equal domain population, while those with $L = 1$ in (c) are calculated with both the domain 1 (D1) only (dashed line) and equal population of all 3 domains (solid line). The solid in (b) is for $H//c$, while the dashed line is for the field with an 10° offset from c-axis. The inset in (c) presents the schematic view of 3 domains(D1-D3) with respect to the field H; only the in-plane field component is shown.

shaped sample with the wide ab plane was held between two quartz stages in a heat shrinkable tube with an inside diameter of 2.5 mm so that the crystallographic c axis is parallel to the cylindrical axis of the tube. The pulsed magnetic field was applied parallel to the cylindrical axis. The absolute value of the high-field magnetization was calibrated with the magnetization measured by the SQUID magnetometer at T = 1.8 K.

The neutron scattering experiment was performed at the HFM/EXED high-field neutron facility at the BER-II research reactor at HZB. The facility combined a horizontal field DC hybrid magnet (HFM) capable of reaching fields up to 26 T and a time-of-flight neutron diffractometer [36–38]. The HFM had 30° conical openings on both ends and could be rotated with respect to the incident neutron beam by an angle $\omega \leq 12°$; a sample rotation around the vertical axis was also implemented which allowed to reach a considerable reciprocal space volume for zero-field conditions or in the case of isotropic systems. The 30° forward scattering direction in the instrument was covered by a position-sensitive detector and was suitable for studying magnetism.

For the neutron scattering experiment the sample had been aligned with the $(0, 0, L)$ direction along the field and $(H, H, 0)$ lying in the horizontal plane and perpendicular to the field. The experimentally determined sample misalignment was about 7° around $[(H, H, 0)]$-axis. For accessing reflections with $L =1$, the sample had been rotated by 18° around the vertical axis. The experiment geometry was calculated by means of the software EXEQ[39]. A sketch of the scattering geometry is shown as an inset in Fig. 2(a). All the measurements were performed at 2 K with a temperature variation of about 0.3 K between different data collection processes.

III. MAGNETIZATION AND NEUTRON DIFFRACTION RESULTS

The magnetization measured in pulsed fields up to saturation is displayed in Fig. 1. To keep the consistency, the green line in Fig.1(a) obtained from the measurements in DC fields shows the data from the same badge sample as that used in neutron scattering experiment. As one can see the magnetization measured with DC and pulsed fields shows a very good quantitative agreement. Two transitions at $\sim$ 12T and around $\sim$ 22T can be identified; hereafter we refer to these two field values as $\mu_0 H_{c1}$ and $\mu_0 H_{c2}$. For the latter transition at the higher field, two samples show slight difference, which might be due to an error in the subtraction of background signal coming mainly from the sample holder. The pulsed field data collected at 1.3K clearly shows a plateau as displayed in Fig. 1(a) and can be resolved more clearly from the derivative. A magnetization jump is observed at 12T, followed by a plateau-like feature with increasing field. Our observation is consistent with previous experimental works [23] and calculation[27], and signifies a transition from the umbrella to the UUD-like phase. The jump magnitude is suppressed by temperature and vanishes when approaching T_N. The temperature dependence of the magnetization around $\mu_0 H_{c1}$ is given in the upper inset of Fig.1(a). Note that at temperatures around 2 K, where neutron measurements have been performed, the plateau-like feature smears profoundly. Moreover, we performed a detailed study of the orientation- and temperature-

dependence for the $\mu_0 H_{c1}$ transition, as shown in Fig. 1(b-c). The transition fields have been extracted by derivation. As one can see, $\mu_0 H_{c1}$ decreases for both the increasing temperature and the angle deviation from the c-axis. At $T = 1.9\ K$, with the field offset from the c-axis by $\sim 20°$, $\mu_0 H_{c1}$ decreases from 12 T down to about 11 T (Fig. 1(b)). Hereafter we name the transition field for the $\sim 20°$ offset as $\mu_0 H'_{c1}$=11T. Around $\mu_0 H_{c2}$, the derivative exhibits a weak peak-like anomaly as indicated in the 1st derivative of Fig. 1(a) for both samples. Such a transition was also recently reported in Ref. [28]. We also note that the H_{c2} transition was not observed in the earlier work Ref. [23]. The main difference between ours and Susuki's et al experiment is the following: We have used only one well aligned single crystal while in Ref.[23] about ten single crystals had been stacked together with an orientation dispersion of about 10°. Since recent experiments show that H_{c2} transition field increases with field offset quickly [40], we assume that the magnetization anomaly was smeared out by the distribution of the critical fields due to the crystal orientation dispersion. The transition fields for both samples are slightly different, which might be caused by small differences in sample alignment or to be a sample property.

To shed light on the spin ground state evolution of $Ba_3CoSb_2O_9$ as a function of the magnetic field along the c-axis, we have measured the intensity of several accessible nuclear and magnetic reflections. In the current experimental setup with field approximately along the c-axis, several reflections with L=0 and 1 can be reached, namely the magnetic (-1/3, -1/3, 0), (1/3, -2/3, 0), (-2/3, -2/3, 1) and the nuclear (-1, 0, 0). Due to the very restrictive instrument geometry, the sample has to be rotated by an angle with respect to both the field and incident beam directions in order to access a given reflection. For the L=0 reflections, the field is applied along $[0, 0, L]$ direction with about 7° deviation, while for the (-2/3, -2/3, 1) reflection, the angle has be increased up to $\sim$18°, i.e. the field is applied 18° off the c-axis. Due to rather small (7°) angular offset, hereafter the former setup is referred to as $H \parallel c$ case.

For $H \parallel c$ several reflections (-1, 0, 0), (-1/3, -1/3, 0) and (1/3, -2/3, 0) have been measured as shown in Fig. 2(a-b). The latter two reflections are symmetric with respect to the field along the c-axis, ignoring a small field offset. For (-1, 0, 0) reflection, after subtraction of the nuclear contribution, the magnetic signal shows monotonous increase with field, reflecting the development of a ferromagnetic component in the system. A fit of the intensity I to a quadratic function $I(H) = aH^2+b$, with a and b being constants, can depict the curve very well (not shown), demonstrating a linearly increasing ferromagnetic component $M(H)$ along c-axis with field, H, consistent with the magnetization measurements.

Purely magnetic (-1/3, -1/3, 0) and (1/3, -2/3, 0) reflections exhibit more complex behavior with field. Below $\mu_0 H_{c1}$ no visible intensity can be observed. This is consistent with the zero field structure, in which the antifer-

romagnetic interlayer ordering along the c-axis leads to the presence of (H, K, L) reflections with $L = 2n+1$ and absence of the $L = 2n$ ones where n is an integer. Up to $\mu_0 H_{c1}$, the absent (-1/3, -1/3, 0) and (1/3, -2/3, 0) reflections indicate that the interlayer magnetic order is still antiferromagnetic, consistent with the umbrella phase. The abrupt emergence of (-1/3, -1/3, 0) and (1/3, -2/3, 0) at $\mu_0 H_{c1}$ signifies a transition to a phase where the inversion symmetry of the antiferromagnetic components between adjacent layers is broken. With further increase of the field, the intensity saturates at about 18T and then starts decreasing with a kink around 22.5 T. The latter indicates a phase transition, corresponding to the transition in the magnetization around 22 T, namely $\mu_0 H_{c2}$. In the field range up to the maximum available in this experiment 25.9 T, the intensity decreases continuously. To verify if there is a field history dependence, we performed measurements for both the up and down field ramps. No hysteresis has been observed for both reflections. Moreover, both (-1/3, -1/3, 0) and (1/3, -2/3, 0) show the same field dependence and are very close in magnitude, confirming these two reflections remain equivalent in high fields.

The $L=1$ reflection, with field oriented 18° off the c-axis, also exhibits a complex behavior as shown in Fig. 2(c). This reflection exists already at zero field in agreement with the AFM order along the c-axis. Up to 11 T, the intensity slightly increases with the field, followed by a jump after which a monotonous decrease is observed. This jump in intensity corresponds to the $\mu_0 H'_{c1}$ transition in the magnetization measurements (Fig. 1(b)). Around 22 T, the reflection intensity becomes very weak, making any further transitions at higher fields undetectable. The field ramp up and down processes shows the same result, i.e. within the experimental resolution no hysteresis is observed.

IV. THEORETICAL CALCULATION

Our experiment offers a unique opportunity to gain deeper insight into the ground state of TLHAF in a field along the c-axis. Several transitions have been unambiguously observed by the measurement and their relation to the magnetic reflections has been established. Despite all these, a proper determination of the corresponding magnetic structures is not feasible due to the very limited number of the reflections we could reach. As a result, to interpret the data, we use a theoretical approach. The calculations are performed under the same theoretical framework as we used in our previous work for H in the ab-plane[30], which is the CMF+S method for the following S $= 1/2$ XXZ model of stacked weakly coupled triangular layers [22, 25, 27, 30]:

$$\hat{\mathcal{H}} = \sum_{\langle i,j \rangle} \left[J\left(\hat{S}_i^x \hat{S}_j^x + \hat{S}_i^y \hat{S}_j^y \right) + J_z \hat{S}_i^z \hat{S}_j^z \right]$$
$$+ \sum_{\langle i,l \rangle'} \left[J'\left(\hat{S}_i^x \hat{S}_l^x + \hat{S}_i^y \hat{S}_l^y \right) + J_z' \hat{S}_i^z \hat{S}_l^z \right]$$
$$- \boldsymbol{H} \cdot \sum_i \hat{\boldsymbol{S}}_i \qquad (1)$$

with the intralayer (J, J_z) and interlayer (J', J_z') nearest-neighbor couplings. The CMF+S method takes into account the in-plane quantum fluctuation effects via the extrapolation with respect to the size of the clusters on the triangular-lattice (ab) planes [25, 30].

In the CMF+S analysis, we employ the triangular-shaped clusters of $N_C = 21, 28, 36$ sites. The intralayer interaction between a cluster-edge spin and its neighboring spin at an out-of-cluster site with sublattice index μ is replaced by an effective magnetic field $\left(J m_\mu^x, J m_\mu^y, J_z m_\mu^z \right)$ acting on the edge spin [41, 42]. The small interlayer couplings are treated within the standard mean-field approximation [25, 30]. Under the $3 \times 2 = 6$ sublattice ansatz $(\mu = A, B, C, A', B', C')$, we calculate the sublattice magnetic moments $\boldsymbol{m}_\mu$ by solving the set of six self-consistent equations

$$\boldsymbol{m}_\mu = \frac{3}{N_C} \sum_{i_\mu} \langle \hat{\boldsymbol{S}}_{i_\mu} \rangle \quad (\mu = A, B, C, A', B', C') \qquad (2)$$

To calculate the ground-state expectation values $\langle \hat{\boldsymbol{S}}_{i_\mu} \rangle$, we solve the N_C-site cluster problems by applying the density matrix renormalization group (DMRG) method [43]. The dimension of the truncated matrix product states in DMRG is taken to be sufficiently large for a good convergence of $\boldsymbol{m}_\mu$ (within $\lesssim 10^{-8}$). We calculate all the sublattice magnetic moments $\boldsymbol{m}_\mu$ in a self-consistent way for each cluster size $(N_C = 21, 28, 36)$, and finally perform extrapolation to the infinite cluster size $(N_C \to \infty)$ based on the scaling parameter λ, following the same procedure as Refs. [25, 30].

In the model Hamiltonian (1), the xyz coordinate system is defined with respect to the magnetic unit cell, $\sqrt{3}a \times \sqrt{3}a \times c$, as follows: $H \parallel z$, $x \parallel [H, H, 0]$ and $y \perp x \perp z$, the 18° offset lies in $S_x - S_z$ plane toward x-axis. First, we determined the parameters J, J_z, J', J_z' in Eq. (1) by comparing the calculated magnetization curve $M(H) = (m_A^z + m_B^z + m_C^z + m_{A'}^z + m_{B'}^z + m_{C'}^z)/6$ with the experimental observation for $\boldsymbol{H} \parallel (0, 0, L)$. We tried two models for the anisotropy in the interlayer interactions: (i) isotropic case $(J_z' = J')$ [25, 27, 30] and (ii) anisotropic case with $J_z'/J' = J_z/J$ [22]. As shown in Fig. 1(a), the anisotropy parameters $J_z/J = 0.75$ for (i) and $J_z/J = 0.755$ for (ii) under the assumption of small interlayer coupling, $J'/J = 0.05$, reproduce well the measured transition point around 12 T. To convert the theoretical units of the magnetic field and the magnetization into tesla and μ_B/Co^{2+}, respectively, we set
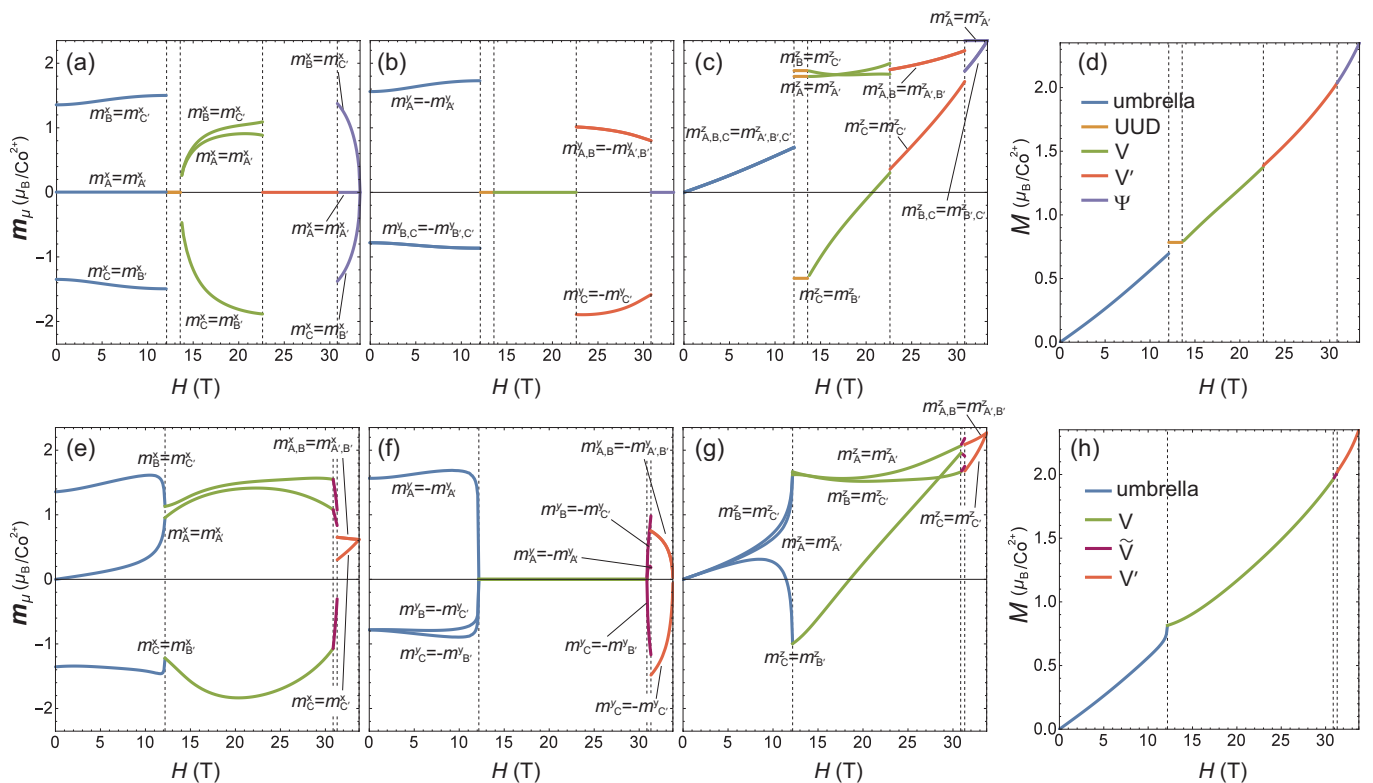
FIG. 3: Calculated magnetic moment components along various directions for three sites in a triangle in a single layer, for field applied along c-axis (a-c) and with $18°$ offset from c-axis (e-g). Derived magnetization as a function of field for various phases for field along c-axis (d) and with $18°$ offset(h).

$J/g\mu_B = 8.655$ [8.57] for (i) [(ii)] and multiply $\boldsymbol{m}_\mu$ by a factor of 4.703, from the fittings of the field strength and magnetization at the saturation. We found that somewhat larger anisotropy is needed to compare with the experiment than those estimated by the other theoretical methods [22, 27]. When changing J'/J (but keeping it small $\lesssim 0.1$), although the value of J_z/J that can reproduce the transition point around 12 T is shifted, e.g., $J_z/J = 0.73$ when $J'/J = 0.025$ for (i), the overall feature of the magnetization curve is almost unchanged. As seen in the lower inset of Fig. 1, the agreement of the magnetization anomaly around 22 T seems to be slightly better when using the model (i) with isotropic interlayer coupling. Therefore, we will use the parameter set $J_z/J = 0.75$, $J'/J = 0.05$, and $J'_z = J'$, throughout the rest of the paper. On the other hand side, the model (ii) cannot be completely ruled out given scatter in the H_{c2} values in two samples under investigation in this work.

Figures 3(a-c) show each component of the calculated sublattice magnetic moments as a function of field with setting $\boldsymbol{H} \parallel (0,0,L)$, and Fig. 3(d) shows the derived magnetization curve $M(H) = (m_A^z + m_B^z + m_C^z + m_{A'}^z + m_{B'}^z + m_{C'}^z)/6$. The selected spin configurations are presented in Fig. 4(a-f). Note that when H is completely parallel to the spin z axis, the model Hamiltonian has

a global rotational symmetry around the field axis, and thus the global azimuthal angle of the spin structure is not fixed. To draw Figs. 3(a-c) and 4(a-f), we chose a certain global azimuthal angle without loss of generality.

The overall transition routine is close to the one obtained from the semiclassical analysis performed in Ref. [27]. Indeed, our CMF+S calculation can be connected and compared with the semiclassical calculation. For $H \parallel a$ in our last work performed by the CMF+S calculation [30], the V and V' phases correspond to the UIF and HF phases shown in Fig.4 of Ref. [27], respectively. In the present work for (nearly) $H \parallel c$, the V (Fig.4(d)) and V'(Fig.4(e)) phases correspond to the LIF and HF phases, respectively. The transition fields between various phases are quantitatively different due to different methods and parameters. Another main difference is that the semiclassical analysis gives no UUD phase when the field is applied along c-axis, while the CMF+S method still predicts a narrow UUD phase (Fig.4(c)) directly following the umbrella phase, even in the presence of the easy-plane anisotropy, $J_z/J = 0.75$. This UUD phase survives merely in a much narrower field range than in the in-plane field case and smears quickly due to a tilting of field and temperature effect. In addition, the CMF+S method with the present values of the parameters predicts the so-called Ψ (or π-coplanar) phase
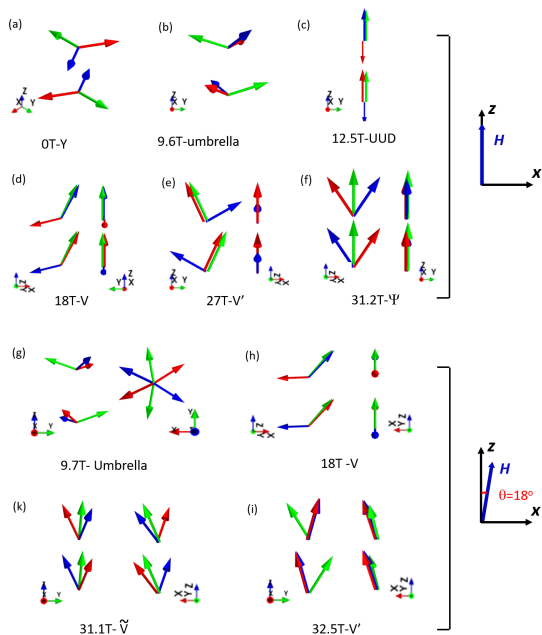
FIG. 4: (color online) the calculated magnetic structure at selected fields for various phase with $H \parallel c$ (a-f) and offset by $18°$ (g-i). The different colors represent various pairs of sites in a sublattice. The $x-y$ plane corresponds to the ab-plane of lattice.

(Fig.4(f)) [42, 44, 45] near the saturation, although its existence strongly depends on the value of the interlayer coupling [25].

For the $H \parallel c$ case, the calculation predicted several transitions to occur at fields 12T, 13.6T, 22.6T, and 30.8T, respectively. We associate the 12 T and 22.6 T transitions with $\mu_0 H_{c1}$ and $\mu_0 H_{c2}$ in experiment, respectively. The predicted narrow UUD phase (Fig.4(c)) in between 12T and 13.6T seems to smear in the experiment at finite temperatures but the tendency towards the formation of the magnetization plateau can be seen in the inset of Fig. 1(a).

For the field offset from the c-axis by $18°$, we present the calculated structure in Fig.3(e-g) and Fig.4(g-i), as well as the derived magnetization curve $M(H) = \cos(\pi/10)(m_A^z + m_B^z + m_C^z + m_{A'}^z + m_{B'}^z + m_{C'}^z)/6 + \sin(\pi/10)(m_A^x + m_B^x + m_C^x + m_{A'}^x + m_{B'}^x + m_{C'}^x)/6$ in Fig.3 (h). Here, we used the same conversion factors as in the case of $H \parallel c$ assuming a small anisotropy in the g factor. The UUD and Ψ phases disappear due to the small field offset from the c-axis. An additional noncoplanar phase, we name it $\tilde{V}$ phase (Fig.4(k)), is predicted in this field orientation, following with V phase (Fig.4(h)) and exists in a narrow field range around 31 T. In the semiclassical calculation [27], this phase (UIF phase) appears with field deviating from a axis and diminishes when field end up with $\sim 18°$ from c axis. In the CMF+S calculation

with $J_z/J = 0.75$ and $J'/J = 0.05$, we found that this phase can pertain up to $\sim 10°$ from c-axis. Moreover, one should note that the umbrella, V, and V' phases all get deformed by an asymmetric field. The deformed-umbrella (Fig.4(g)) and deformed-V(Fig.4(h)) states are now smoothly connected on the magnetization curve. For such an asymmetric field, the ordering plane is locked by the field. For deformed-V state the moments lies in the $S_z - S_x$ plane while the deformed-V'(Fig.4(i)) state sits almost perpendicular to the x axis.

V. DISCUSSION

To compare our experimental results with the theoretically calculated structures, we calculated the intensities of the given reflections as function of field. Generally, the scattering cross section is calculated as

$$\frac{d\boldsymbol{\sigma}}{d\boldsymbol{\Omega}} = \frac{1}{N_m}\frac{2\pi^3}{\nu_0}\sum_{\boldsymbol{\tau}_i}$$
$$\delta(\boldsymbol{Q} - \boldsymbol{\tau}_i)|\hat{\boldsymbol{Q}} \times \hat{\boldsymbol{F}}_M(\boldsymbol{\tau}_i) \times \hat{\boldsymbol{Q}}|^2 \quad (3)$$

where

$$\hat{\boldsymbol{F}}_M(\boldsymbol{Q}) = \gamma r_0 \sum_{\mu} f_\mu(\boldsymbol{Q})\langle \boldsymbol{m}_\mu\rangle e^{i\boldsymbol{Q}\cdot\boldsymbol{r}_\mu}e^{-W_\mu(\boldsymbol{Q})} \quad (4)$$

in which $\gamma = 1.9132$, $r_0 = e^2/(m_e c^2) = 2.8179 \times 10^{-15}$m is the classical radius of electron. N_m is the number of magnetic ions in each magnetic unit cell, ν_0 is the volume of magnetic cell, $\boldsymbol{\tau}_i$ denotes the magnetic propagation vectors, μ is the position of the magnetic atom within a magnetic cell, $f_\mu(\boldsymbol{Q})$ is the atomic form factor of Co^{2+}, $\langle \boldsymbol{m}_\mu\rangle = (m_x, m_y, m_z)_\mu$ describes the magnetic moment vector, $\hat{\boldsymbol{Q}}$ is a unit vector along $\boldsymbol{Q}$ direction and W_j is Debye-Waller factor. The results have been also verified against the FullProf software[46].

To reproduce the intensity correctly, however, the magnetic domain distribution in the real sample has to be taken into account [47]. Multiple domains might affect the intensity of a magnetic reflection, which becomes especially crucial as the domain population can be altered by an external field. Owing to the threefold rotational symmetry about the c-axis in $Ba_3CoSb_2O_9$, there are three magnetic domains (D1-D3) separated by $120°$, as shown in the inset of Fig. 2(c). As the field direction does not exactly coincide with the c-axis, the domain population may vary with field. The nuclear reflection (-1, 0, 0) is not sensitive to that, since the ferromagnetic component is always along the c-axis. On the other hand, the antiferromagnetic reflections show a strong dependence on the domain population. For the reflections (-1/3, -1/3, 0) and (1/3, -2/3, 0), the intensities are sensitive to the domain population only in the V phase, while for the (-2/3, -2/3, 1) reflection in all the magnetic phases.

The domain population thus is the key parameter to be accounted when comparing the theoretical and experimental magnetic intensities. Our choice is based on the following argument. If the field is exactly along the c-axis or with only a small deviation ($\theta = 7°$), an equal population of 3 domains is favorably assumed. However, if a considerable deviation from the c-axis exists, the 3 domains become unequal and various population combinations need to be tested and compared with the experiment. Indeed, the domain with ferromagnetic component located in the plane formed by the field and the c-axis ($X - Z$ plane), i.e., D1 in inset of Fig. 2(c), should be preferred. Furthermore, for a considerable field direction deviation such as $\theta = 18°$ for the $L = 1$ configuration, the in-plane field component changes with field as $H\sin\theta$. The population therefore can also change with the field. It is thus difficult to account for the real configuration in a varying in-plane field. For simplicity, we display the intensity of both the equal population and the only preferred domain. The real configuration must fall in between these two extreme cases.

The obtained intensities for the measured reflections are shown in Fig. 2 as lines. Generally, the calculated results capture the main experimental features quite well, though the quantitative agreement is not always satisfying. For the $L = 0$ reflections (Fig. 2(b)), the transition fields μ_0H_{c1} and μ_0H_{c2} are reproduced. In the intensity calculations, we ignore the small field offset by $\sim 7°$ and assume that the domains are equally populated. This is supported by the observation that two reflections (-1/3, -1/3, 0) and (1/3, -2/3, 0) do not split in the V-phase, which would be the case otherwise. In Fig. 2(b), the transition observed at μ_0H_{c1} for (-1/3, -1/3, 0) and (1/3, -2/3, 0) reflections corresponds to the transition from the umbrella to the coplanar V-phase. We do not clearly observe the plateau UUD-like phase presumably because of the $\sim 7°$ field offset and relatively high (around 2 K) sample temperature, the result which is supported by the bulk measurements as shown in Fig. 1. The same is true for the (-1,0,0) reflection visualized in Fig. 2(a). Here, one can see that the ferromagnetic component increases with field as expected and agrees with the experiment quite well. The anomaly observed at μ_0H_{c2} for (-1/3, -1/3, 0) and (1/3, -2/3, 0) reflections in Fig. 2(b) marks a transition from the V to V' phase, which should be a first order transition according to the theory. Nonetheless, the observed transition shows only a weak anomaly, in contrast to a large jump predicted by the calculations. To examine the effect of $\sim 7°$ offset, as a comparison, we also performed the structure calculation for an offset of 10° as displayed in Fig. 2(b). One can see the offset suppress both UUD phase and also the intensity jump near μ_0H_{c2} as predicted for $H \parallel c$. This implies the observed weak change around μ_0H_{c2} could be ascribed to the offset of field with respect to c-axis. We note a similar discrepancy was also observed in the NMR experiment [27]. Both these inconsistencies suggest the nature of this transition has not been captured correctly. Recently, the magne-

tization and calorimetry experiments suggested that the phase above μ_0H_{c2} could be a Ψ phase rather than a V' phase, since it shows a weak anomaly at the second order transition [28]. Unfortunately, these two phases are indistinguishable from neutron scattering. Here we use the calculated V' phase for the intensity estimation.

Finally we are coming to a discussion of the $L = 1$ reflection measured with a field deviation of 18°, i.e., the antiferromagnetic (-2/3, -2/3, 1) reflection. In this geometry, the U(1) symmetry is broken due to the field offset, therefore the varying domain population has to be considered. We have calculated both the single D1 and the 3 equally populated domain configurations, as shown in Fig. 2(c) by the solid and dashed line, respectively. The transition at $\mu_0H'_{c1}$ is reproduced quite well in both configurations. At low fields, i.e. in the deformed umbrella phase(Fig. 4(g)), the calculations shows the increasing (-2/3, -2/3, 1) intensity consistent with the experimental observation. Above the umbrella phase, the theory predicts the deformed V-phase(Fig. 4(h)). The plateau UUD-like phase is suppressed due to the field tilted off the c-axis. According to the calculations, the deformed V phase is a coplanar phase lying in the $S_x - S_z$ plane ($X - Z$ in Fig. 2(c)), while the deformed V' coplanar phase lies in the $S_z - S_y (Y - Z)$ plane, as shown in Fig. 4(g) and (i), respectively. The calculated transition field $\mu_0H'_{c1} \sim 12T$ is close to that measured by neutron diffraction and magnetization ($\sim 11T$). Both transitions observed in the neutron and calculated data look like first order transitions, in contrast to the magnetization, where this transition behaves more like second order. Above $\mu_0H'_{c1}$, both the experiment and calculation curves decrease linearly with field. We note that the observed intensity of the (-2/3, -2/3, 1) reflection in between 11 and 22.5 T shows a faster decrease than that in the calculation. Beyond $\mu_0H'_{c1}$, the single domain D1 configuration seems to better describe the experimental results, proving a crossover from equal domain to single domain population with increasing in-plane field. Particularly the D1-only configuration shows a similar decreasing slope as that in the experiment for the deformed V-phase. Above 22.5T, the observed intensity vanishes, within the limits of the experimental precision. We therefore cannot verify if the predicted transition from the deformed V to $\tilde{V}$ and $\tilde{V}$ to deformed V' phases occurs in field range 22.5T and higher, which more than 30T (Fig. 3(h)). According to the theory, the deformed V and V' phases are both predicted to be coplanar phases which are not confined in the ab-plane. We infer that the anisotropy in $Ba_3CoSb_2O_9$ system will be gradually suppressed in high fields, and the system will adopt a similar structure as that for $H \parallel ab$ [25, 27].

We note that the discrepancy between the experiment and calculation may be partially ascribed to the inaccurate domain population assumption. In our calculation, a fixed unequal domain population is assumed for the whole field range. However, the population does not likely remain constant as the field is varying. Especially this assumption will fail in the highest field range where

only one domain will be realized. Furthermore, relatively high temperature might be another factor to account for the discrepancy between the experiment and calculation. The experiment has been performed at about 2 ± 0.3 K, which is relatively high temperature considering T_N=3.9K.

VI. CONCLUSION

Using the magnetization measurements up to 35 T, which allowed us to reach saturation, and neutron scattering in fields up to 25.9 T with the field predominately along the c-axis, we have studied the evolution of the ground state of the paradigmatic TLHAF system $Ba_3CoSb_2O_9$. The experimental results are compared with the theoretical calculations based on CMF + S method. The theoretical results are qualitatively consistent with the experimental ones. A transition from the umbrella phase to a coplanar phase at $\mu_0 H_{c1} \sim 12$ T is observed. Below 2K, the magnetization measurements show a narrow UUD-like phase for $H \parallel c$ following the umbrella phase. The UUD-like phase is very sensitive to the field offset from the c-axis and could not be unambiguously observed in the neutron scattering measurements. At $\mu_0 H_{c2} \sim 22.5$ T for $H \parallel c$, a clear transition is observed, which is identified as $V - V'$ transition by our CMF +S calculations. For the 18° field direction offset, we find a transition from a deformed umbrella phase to a deformed V phase at $\mu_0 H'_{c1} \sim$11T. The overall agreement between the experiment and CMF + S calculation is reached. However, one notes the quantitative match between the experiment and the calculations is not as good as it was in the case of the field aligned in the ab-plane [30]. This suggests that further efforts are needed to fully understand the TLHAF system in magnetic fields applied along the c-axis.

VII. ACKNOWLEDGMENTS

[1] P. W. Anderson, Mater. Res. Bull. **8**, 153 (1973).

[2] L. Balents, Nature **464**, 199 (2010).

[3] O. A. Starykh, A. V. Chubukov, and A. G. Abanov, Phys. Rev. B **74**, 180403(R) (2006).

[4] A. L. Chernyshev, and M. E. Zhitomirsky, Phys. Rev. B **79**, 144416 (2009).

[5] M. Mourigal, W. T. Fuhrman, A. L. Chernyshev, and M. E. Zhitomirsky, Phys. Rev. B **88**, 094407 (2013).

[6] E. A. Ghioldi, A. Mezio, L. O. Manuel, R. R. P. Singh, J. Oitmaa, and A. E. Trumper, Phys. Rev. B **91**, 134423 (2015).

[7] E. A. Ghioldi, M. G. Gonzalez, S. Zhang, Y. Kamiya, L. O. Manuel, A. E. Trumper, and C. D. Batista, Phys. Rev. B **98**, 184403 (2018).

[8] D. A. Huse, and V. Elser, Phys. Rev. Lett. **60**, 2531 (1988).

[9] T. Jolicoeur, and J. C. Le Guillou , Phys. Rev. B **40**, 2727 (1989).

[10] B. Bernu, P. Lecheminant, C. Lhuillier, and L. Pierre, Phys. Rev. B **50**, 10048 (1994).

[11] R. R. P. Singh, and D. A. Huse, Phys. Rev. Lett. **68**, 1766 (1992).

[12] L. Capriotti, A. E. Trumper, and S. Sorella, Phys. Rev. Lett. **82**, 3899 (1999).

[13] W. H. Zheng, J. O. Fjærestad, R. R. P. Singh, R. H. McKenzie, and R. Coldea, Phys. Rev. B **74**, 224420 (2006).

[14] S. R. White, and A. L. Chernyshev, Phys. Rev. Lett. **99**, 127004 (2007).

[15] T. Ono, H. Tanaka, H. Aruga Katori, F. Ishikawa, H. Mitamura, and T. Goto, Phys. Rev. B **67**, 104431 (2003).

[16] N. A. Fortune, S. T. Hannahs, Y. Yoshida, T. E. Sherline, T. Ono, H. Tanaka, and Y. Takano, Phys. Rev. Lett. **102**, 257201 (2009).

[17] Y. Shirata, H. Tanaka, A. Matsuo, and K. Kindo, Phys. Rev. Lett. **108**, 057205 (2012).

[18] H. D. Zhou, C. Xu, A. M. Hallas, H. J. Silverstein, C. R. Wiebe, I. Umegaki, J. Q. Yan, T. P. Murphy, J.-H. Park, Y. Qiu, J. R. D. Copley, J. S. Gardner, and Y. Takano , Phys. Rev. Lett. **109**, 267206 (2012).

[19] A. Sera, Y. Kousaka, J. Akimitsu, M. Sera, T. Kawamata, Y. Koike, and K. Inoue, Phys. Rev. B **94**, 214408 (2016).

[20] A. Sera, Y. Kousaka, J. Akimitsu, M. Sera, and K. Inoue, Phys. Rev. B **96**, 014419 (2017).

[21] Y. Doi, Y. Hinatsu, and K. Ohoyama, J. Phys.: Condens. Matter **16**, 8923 (2004).

[22] Y. Kamiya, L. Ge, T. Hong, Y. Qiu, D. L. Quintero-Castro, Z. Lu, H. B. Cao, M. Matsuda, E. S. Choi, C. D. Batista, M. Mourigal, H. D. Zhou, and J. Ma, Nat. Commun. **9**, 2666 (2018).

[23] T. Susuki, N. Kurita, T. Tanaka, H. Nojiri, A. Matsuo, K. Kindo, and H. Tanaka, Phys. Rev. Lett. **110**, 267201 (2013).

[24] J. Ma, Y. Kamiya, T. Hong, H. B. Cao, G. Ehlers, W. Tian, C. D. Batista, Z. L. Dun, H. D. Zhou, and M. Matsuda, Phys. Rev. Lett. **116**, 087201 (2016).

[25] D. Yamamoto, G. Marmorini, and I. Danshita, Phys. Rev. Lett. **114**, 027201 (2015).

[26] G. Quirion, M. Lapointe-Major, M. Poirier, J. A. Quilliam, Z. L. Dun, and H. D. Zhou, Phys. Rev. B **92**, 014414 (2015).

[27] G. Koutroulakis, T. Zhou, Y. Kamiya, J. D. Thompson, H. D. Zhou, C. D. Batista, and S. E. Brown , Phys. Rev. B **91**, 024410 (2015).

[28] N. A. Fortune, Q. Huang, T. Hong, J. Ma, E. S. Choi, S. T. Hannahs, Z. Y. Zhao, X. F. Sun, Y. Takano, and H. D. Zhou, Phys. Rev. B **103**, 184425 (2021).

[29] D. Macdougal, S. Williams, D. Prabhakaran, R. I. Bewley, D. J. Voneshen, and R. Coldea, Phys. Rev. B **102**, 064421 (2020).

[30] X.Z. Liu, O. Prokhnenko, D. Yamamoto, M. Bartkowiak, N. Kurita, and H. Tanaka, Phys. Rev. B **100**, 094436 (2019).

[31] D. J. J. Farnell, R. Zinke, J. Schulenburg, and J. Richter, J. Phys.: Condens. Matter **21**, 406002 (2009).

[32] A. Honecker, J. Phys.: Condens. Matter **11**, 4697 (1999).

[33] T. Sakai, and H. Nakano, Phys. Rev. B **83**, 100405(R)(2011).

[34] C. Hotta, S. Nishimoto, and N. Shibata, Phys. Rev. B **87**, 115128 (2013).

[35] S. Ito, N. Kurita, H. Tanaka, S. Ohira-Kawamura, K. Nakajima, S. Itoh, K. Kuwahara, and K. Kakurai, Nat. Commun. **8**, 235 (2017).

[36] O. Prokhnenko, P. Smeibidl, W.-D. Stein, M. Bartkowiak, and N. Stüsser, Journal of Large Scale Research Facilities JLSRF **3**, A115 (2017).

[37] P. Smeibidl, M. Bird, H. Ehmler, I. Dixon, J. Heinrich, M. Hoffmann, S. Kempfer, S. Bole, J. Toth, O. Prokhnenko, and B. Lake, IEEE Trans. Appl. Supercond. **26**, 4301606 (2016).

[38] O. Prokhnenko, W. Stein, H. Bleif, M. Fromme, M. Bartkowiak, and T. Wilpert, Rev. Sci. Instrum. **86**, 033102 (2015).

[39] M. Bartkowiak, K. Prokes, M. Fromme, A. Budack, J. Dirlick, and O. Prokhnenko, J. Appl. Crystallogr. **53**, 1613 (2020)

[40] Okada, Tanaka, Kurita, Yamamoto, Matsuo and Kindo, in preparation

[41] D. Yamamoto, A. Masaki, and I. Danshita, Phys. Rev. B **86**, 054516 (2012).

[42] D. Yamamoto, G. Marmorini, and I. Danshita, Phys. Rev. Lett. **112**, 127203 (2014);

[43] D. Yamamoto, G. Marmorini, M. Tabata, K. Sakakura, and I. Danshita, Phys. Rev. B **100**, 140410(R) (2019).

[44] O. A. Starykh, W. Jin, and A. V. Chubukov, Phys. Rev. Lett. **113**, 087204 (2014).

[45] D. Yamamoto, H. Ueda, I. Danshita, G. Marmorini, T. Momoi, and T. Shimokawa, Phys. Rev. B **96**, 014431 (2017).

[46] J. J. Rodriguez-Carvajal, Physica B. **192**, 55 (1993).

[47] T. Nakajima, S. Mitsuda, T. Haku, K. Shibata, K. Yoshitomi, Y. Noda, N. Aso, Y. Uwatoko, and N. Terada, J. Phys. Soc. Japan **80**, 014714 (2011)